PROCESSING OF POROUS CERAMICS – A CASE STUDY WITH HYDROXYAPATITE AND PLANTAGO OVATA

A THESIS SUBMITTED IN PARTIAL FULFILMENT OF

THE REQUIREMENT FOR THE DEGREE OF

B.Tech in Ceramic Engineering

By

Sidhartha Sankar Rout (110CR0441)

Under the guidance of Prof. Santanu Bhattacharyya

Department of Ceramic Engineering

National Institute of Technology, Rourkela

2014

DEPARTMENT OF CERAMIC ENGINEERING

National Institute of Technology,

Rourkela-769008

CERTIFICATE

This is to certify that the thesis entitled, "PROCESSING OF POROUS CERAMICS – A CASE STUDY WITH HYDROXYAPATITE AND PLANTAGO OVATA" submitted by Sidhartha Sankar Rout in partial fulfillment of the requirement for the award of Bachelor of Technology Degree in Ceramic Engineering at the National Institute of Technology, Rourkela is an authentic work carried out by him under my supervision and guidance. To the best of my knowledge, the contents embodied in the thesis has not been submitted in any other University/Institute for the award of any Degree or Diploma.

Date:

S.BHATTACHARYYA

Dept. of Ceramic Engineering

National Institute of Technology

Rourkela - 769008

ACKNOWLEDGEMENT

I wish to express my sincere thanks to **Prof. S. Bhattacharyya,** Department of Ceramic Engineering, N.I.T. Rourkela for assigning me the project "PROCESSING OF POROUS CERAMICS – A CASE STUDY WITH HYDROXYAPATITE AND PLANTAGO OVATA" and for his guidance, criticism and suggestions throughout this project work.

I would like to express my gratitude to **Prof. S. K. Pratihar and Prof. J. Bera** for their valuable suggestions and motivations at various stages of the work.

Last but not least, my solemn thanks to all other faculties, staffs and friends who have patiently extended all sorts of help for achieving this undertaking.

Sidhartha Sankar Rout

B.Tech Ceramic Engineering

CONTENTS

LIST OF FIGURES

ABSTRACT

The present study dealt with the processing and characterization of porous ceramics using Plantago ovata as pore former. Hydroxyapatite was chosen as the base ceramic matrix for creation of pores. The hydroxyapatite powder was prepared by wet chemical method using diammonium hydrogen phosphate and calcium nitrate. The calcined (at 850℃) powder was predominantly hydroxyapatite. Porosity in hydroxyapatite compacts were generated on firing pellets of hydroxyapatite and Plantago ovata at 1250℃ and 1300℃. Different volume fraction (0, 1.1, 2.2, 10.5, 20, 28, and 36%) of Plantago ovata was added as porogen. The porosity developed did not follow a linear relationship with pore former. Maximum porosity (42.62%) was recorded at 36 vol% Plantago ovata addition. CCS followed a decreasing trend with increasing pore former vol%. The highest CCS was 56.53 MPa at 0% addition and lowest (3.795MPa) at 36% addition. FESEM images show that both macro and micro porosities are present. The images also indicate that an increase in pore former vol% leads to larger pore size and more porous samples.

CHAPTER 1

INTRODUCTION

INTRODUCTION

Due to their complex crystal structural and predominantly covalent bonding ceramic materials show some unique properties like hardness, melting point and corrosion resistance etc. Such ceramics find many applications starting from advanced heat engines to transmission of information. In traditional ceramics the fabrication is made from low cost natural raw material which makes it difficult for microstructural control, and leads to compositional heterogeneities, other processing defects and unreliable properties. Therefore, since majority of ceramic processing involve powder, forming process involving powders are more relevant rather than melt casting and other processing techniques. Liquid precursor techniques like sol gel processing suffer from large volume variation during drying and sintering and this factor limits the applicability of this technique to shaping small bodies. Most advanced ceramics are prepared as powder compacts followed by densification through sintering. Recently many conventional and non-conventional processing routes have been adapted like gel casting [1, 2], near net shape forming [3], solid free form processing [4] etc. Among both the traditional and advanced ceramics, porous ceramic occupy a distinct position because of certain unique and remarkable properties it imparts whenever pores and void spaces are intentionally introduced in the body during its processing. The following section describes in detail the different types of porous ceramics, their processing and application areas.

1.1 Porous Ceramics

1.1.1 What are porous ceramics?

Porous Ceramics are classified as those ceramics having porosity 20-95%. Depending on the fabrication process, these ceramics can have either open or closed pores or a combination of both while open pores are open to the surface while closed pores are sealed from the surface. Both the pore types can also be either interconnected or isolated pores.

Porous ceramics have been classified on the basis of (a) volume fraction porosity, (b) nature of porosity (c) Size of Pores. On the basis of pore size porous ceramics can be classified as microporous (less than 2nm), mesoporous (2-50nm), and macroporous (greater than 50nm).

Cellular ceramics can also be classified as honey- combs and foams. In honeycomb structure, the cells form as an array in honey- comb, whereas foams consist of a 3-dimensional array of hollow polygons. Foams are usually sub-divided into two further categories, depending on whether or not the individual cells possess solid faces. The material is termed open-cell, if the solid of which the foam is prepared is contained only in cell edges. The foam is termed closed-cell if the cell faces are present and the individual cells are isolated from each other. In general, foams can be partly closed and partly open. [5]

1.1.2 Importance, Properties and Applications

Porous ceramic materials offer a combination of various properties which make them to be used in wide gamut of technical applications. Some of those are low thermal conductivity [6, 7], and high thermal shock resistance [8]. The thermal conductivity and effusivity (rate at which material can absorb heat) are dependent on porosity, i.e. they decrease as the porosity increases. [9]

Porous ceramics have been used as filters for the cleaning [10], separation of materials in food and chemical sectors [11, 12]. They have special properties like resistance to aging in operation and to high pressure, good permeability [13] and high reliability. [14]

In the preceding sections, the basic concept of porous ceramics, its applications, classification have been discussed. Since the present work involves the processing of porous ceramics. Therefore hydroxyapatite was chosen as the base material in which porosity was chosen to be created. The following sections therefore discuss the properties of hydroxyapatite.

1.2 Hydroxyapatite

Natural hydroxyapatite $Ca_{10}(PO_4)_6(OH)_2$ (carbonated apatite) forms an important bone constituent. Excellent bio-compatibility in bone contact along with its similarity in chemical composition with the natural bone material also leads to the use of synthetic hydroxyapatite implant material. Porous Hydroxyapatite also has been used in biomedical field including bone tissue regeneration, cell development applications, and drug delivery. [15] In bone tissue engineering it has been applied as bone filler material, artificial bone graft material, and in prosthesis revision surgery. Porous hydroxyapatite is more resorbable and more osteo-conductive than its denser counterpart and in porous form the surface area is greatly enhanced which allows more cells to be carried in comparison with dense HA. [16]

1.2.1 Atomic Structure of Hydroxyapatite (HA)

Hydroxyapatite (HA) belongs to the apatite group and has the composition $Ca_{10}(PO_4)_6(OH)_2$. HA has a hexagonal structure (sp. gr. P63/m, two formula units per unit cell) with lattice parameters a = 0.942 nm and c = 0.687 nm. [17] The ideal formula of HA is $Ca_{10}(PO_4)_6(OH)_2$. The atomic structure of HA and its projection along the c axis are shown in Fig.

1.1. The Calcium atoms reside in two positions: six atoms per unit cell are in position Ca(II) and four atoms are in position Ca(I). Ca(I) is located on the threefold axis and is coordinated by nine oxygen of phosphate groups. The Ca(II) atoms form equilateral triangles.

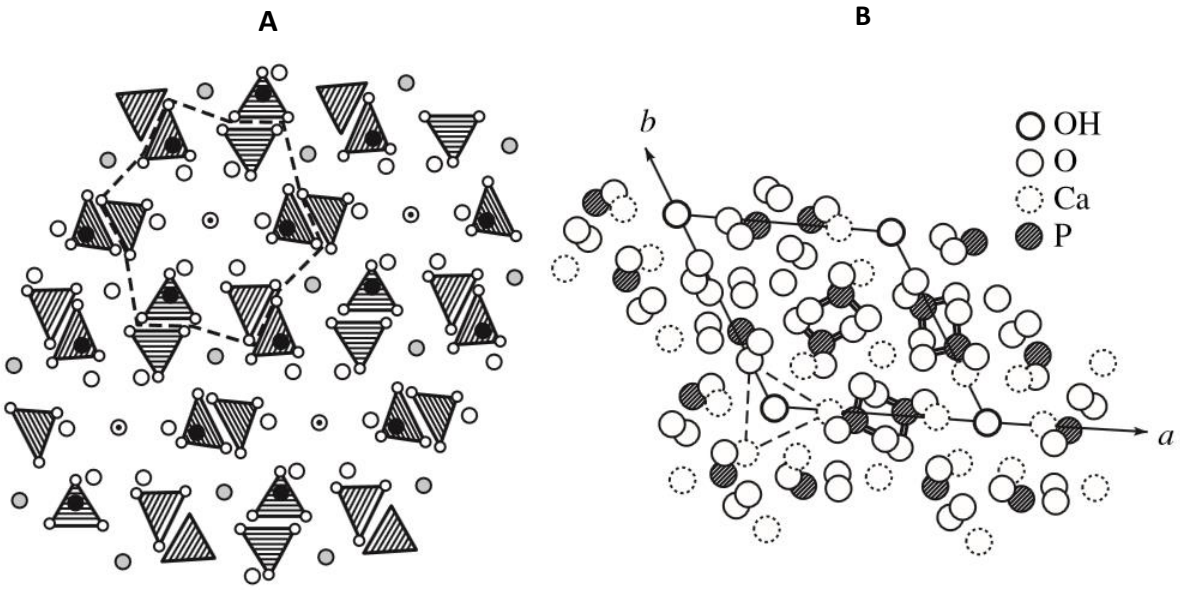

Fig. 1.1 (A) Atomic structure of Hydroxyapatite (HA) and

(B) Its projection along the c axis. [11]

1.3 Properties of Hydroxyapatite (HA)

1.3.1 Biocompatibility

HA is highly biocompatible and therefore it is used in different biomedical applications such as artificial teeth and bone, tissue formation and coatings to improve the biocompatibility and orthopedic growth. [18-ref] HA also acts a protein-binding agent [19], and is therefore used in chromatography and bacterial culture.

1.4 HA based porous ceramics

The evolution of advanced materials for clinical uses is one of the major difficulty facing today's materials engineering. The greatest potential for bone engrafting is exhibited by materials based on hydroxyapatite (HA), $Ca_{10}(PO_4)_6(OH)_2$, which creates strong bonding with bone tissues [20], shows osteo-conductive property [21], is stable towards bio-resorption, and has no unfavorable effects on the human organism. The biological properties of Hydroxyapatite ceramics among other factors depend on their chemical and phase composition, microstructure, pore size, and pore volume.[22] Depending on the bearing mechanical strength of the bone implant, both porous and dense ceramics are used in surgical operations. Low strength porous ceramics are used in drug delivery [23] and as implants in soft tissues which do not go through substantial stresses. Pores in engrafts are required for osteo-integration, and this depends on the pore size, volume, and interconnectivity.

CHAPTER 2

LITERATURE REVIEW

LITERATURE REVIEW

Y Tang et al. studied the processing and pore structure characterization of hydroxyapatite disks [24].The shaped disk samples were formed by the mixture of hydroxyapatite (HAP) powders and mono dispersed polystyrene microspheres. Uniform pore structure with a wide variations in pore size were created by sintering the disks. [24]

Deville et al. [25] studied the freeze drying of hydroxyapatite powders starting with varying slurry concentrations and different sintering conditions. Porous materials with total porosity ranging between 40% to 65% could be obtained by freezing of hydroxyapatite aqueous suspensions following subsequent ice sublimation and sintering. Open and unidirectional porosity exhibited a lamellar morphology. By varying the freezing rate of the slurries and the slurry concentration, size of the pores could be varied. The influence of cooling rate, particle size and slurry concentration were found to affect the pore size, shape and distribution. Due to their lamellar architecture and the pore shape anisotropy, the processed materials exhibited unusually high compressive strength (145MPa for 47% porosity and 65MPa for 56 % porosity material). Thus these material had potential for application as load bearing implants. [25]

Soon-Ho Kwon et al. [26] successfully prepared porous bio-ceramics with variable porosity. The authors used poly urethane sponge process to prepare porous HA, TCP and biphasic HA-TCP. The number of coatings on the sponge struts regulated the porosity. While single coating resulted in 90% porosity with pores being totally interlinked, the porosity dropped 65% when the sintered body was coated for 5 times. [26]

CHAPTER 3

EXPERIMENTAL

EXPERIMENTAL

3.1 Synthesis of Hydroxyapatite

HA was prepared by solution-precipitation method using Calcium Nitrate Tetra-hydrate $Ca(NO_3)_2 \cdot 4H_2O$ and Di-Ammonium hydrogen-phosphate $(NH_4)_2HPO_4$ as the reactant materials and ammonia solution.

The Ca:P ratio for stoichiometric Hydroxyapatite was 1.67. Keeping that ratio constant, the amount of required Di-Ammonium hydrogen-phosphate was calculated and made by dissolving Di-Ammonium hydrogen-phosphate in DI water. The prepared solution of Di-Ammonium hydrogen-phosphate was slowly poured to the Calcium Nitrate Tetra-hydrate solution resulting in turbidity. Concentrated nitric acid was dropwise added to the solution to make the solution clear. 1:1 Ammonia solution was added to the above solution drop wise which resulted in white precipitate of HA. The pH was maintained between 10 to 11.The precipitate was stirred for 2 hours followed by overnight aging. The precipitate were settled followed by decantation of precipitate and removal of ammonia by number of washing of the precipitate with distilled water.

The relevant chemical reaction is:

$$10\ Ca(NO_3)_2.\ 4H_2O + 6\ (NH_4)_2.\ HPO_4 + 8\ NH_4OH = Ca_{10}(PO4)_6(OH)_2 + 20\ NH_4NO_3 + 20\ H_2O$$

(1)

The repeated washing of Hydroxyapatite was affected by centrifugation process at a rotational speed of 8000 rpm. The formed powder was oven dried at 80℃ for 24 hour and fired at 850℃ for 2 hour. Following is the flow chart of the above process:

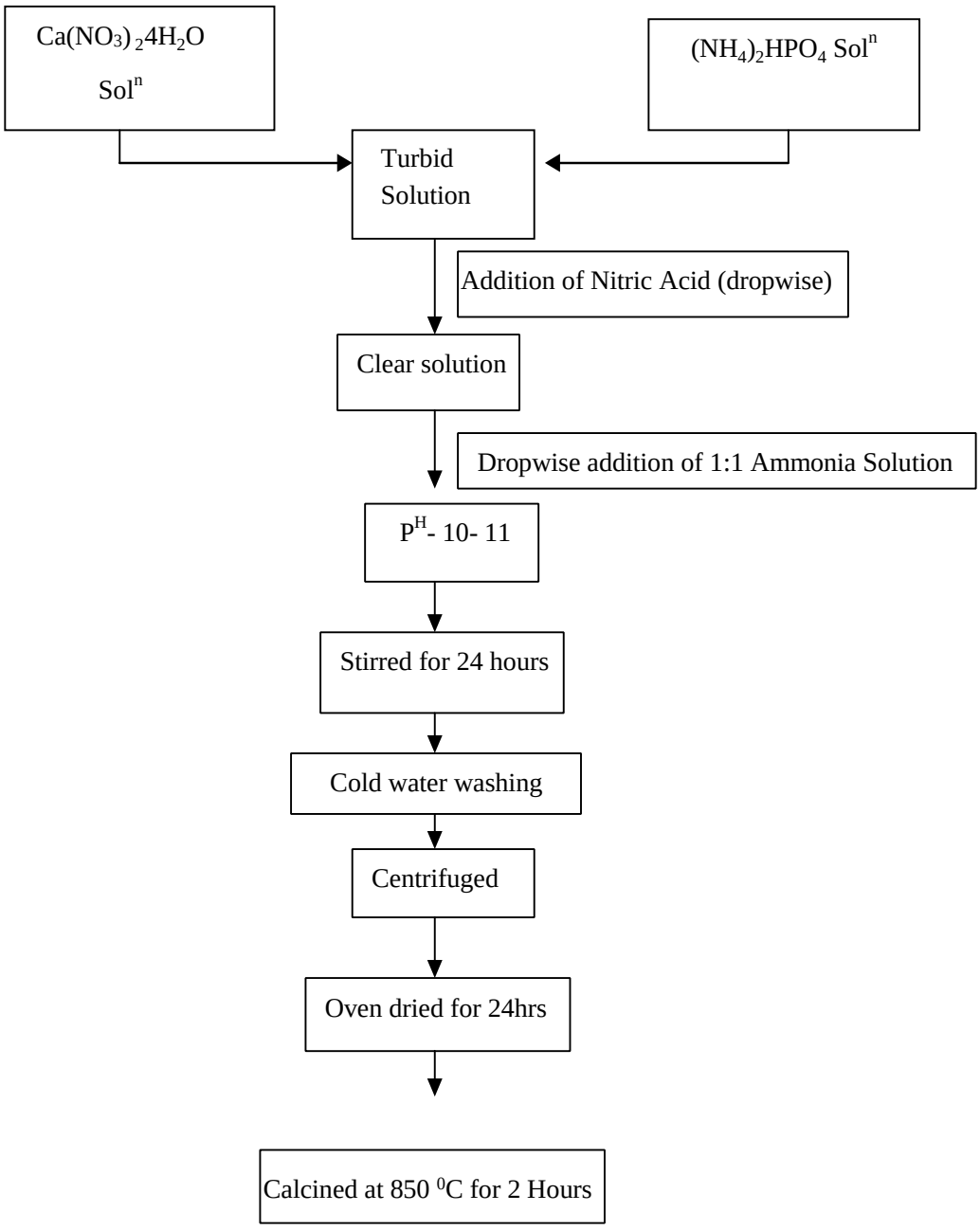

Figure 3.1 Flow Chart for Synthesis of Hydroxyapatite

3.2 Phase Analysis of Hydroxyapatite (HA)

The phases in the calcined powder was studied by XRD (Rigaku Japan/ Ultima-IV X-Ray Diffractometer). The samples were scanned at $20°/\text{min}$ in 2θ range $10° - 80°$. The peaks were matched with the standard HA JCPDS file 74-0565.

3.3 Preparation of Porous HA Pellets

3.3.1 Materials Required:

The starting materials were calcined HA, Plantago ovata

3.3.2 Mixing: *Calcined* hydroxyapatite powder was ground in agate mortar pestle and mixed with Plantago ovata in the ratio as shown in the table -1. 3% PVA as binder was added to it dropwise till the mixture was wet. Then the sample was kept under lamp for 1 hour for drying and reground.

3.3.3 Pressing: Cylindrical pellets were pressed using die (high carbon high chrome) of diameter 12.5 mm in hydraulic press (CARVER UK). The applied load was 3Tons and Dwell Time was 90seconds.

3.3.4 Drying and Sintering: Pellets obtained after pressing were dried in oven at 80^0C for 1 day and then sintered at 1250^0C for 1 hour soaking time and heating schedule of $3℃ / m$in.

Different batches of pellets were prepared as per the weight and volume ratios given below. Corresponding sample IDs were also mentioned.

Table 3.1 Sample ID of HA pellets, corresponding weight% and volume% of Plantago ovata

SI No	**Sample ID**	**Weight percentage of Plantago ovata**	**Volume Percentage Of Plantago ovata**
1	H 100 P0	0	0
2	H 99.5 P0.5	0.5	1.1
3	H 99 P01	1	2.2
4	H95 P05	5	10.5
5	H90 P10	10	20
6	H85 P15	15	28
7	H80 P20	20	36

Flow Chart

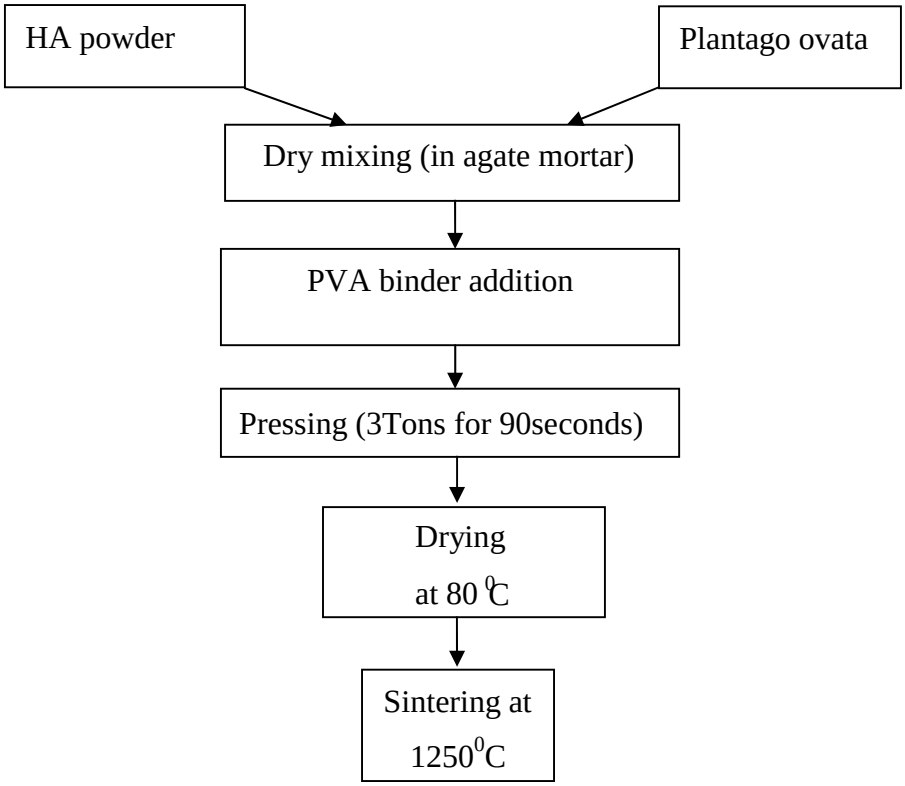

Fig 3.2 Flow chart for preparation of sintered HA Pellets

3.4 Characterizations

3.4.1 Apparent Porosity and Bulk Density Measurement

The apparent porosity and bulk density of sintered HA pellets were measured by Archimedes principle for each batches of prepared pellets. The dry weight of the samples were taken and then samples were immersed in kerosene and evacuated till the bubbles stopped coming out of the pellets. Then the beakers were kept inside the vacuum desiccator for 30minutes. The suspended and soaked weights were taken for each batch.

AP and BD were calculated by the following formulae. [27]

Apparent Porosity = (S-D) / (S-W) (2)

Bulk Density = D / (S-W) (3)

Where, D = Dry weight, W = Soaked weight, S = Suspended weight

3.4.2 Measurement of compressive strength of HA Pellets

The cold crushing strength of the pellets having 12 mm diameter and about 12mm height were measured using Universal testing machine (UTM) Model H10KS Tinius Olsen. The cylindrical pellets were broken by applying compressive force and CCS was calculated using the following formula. [28]

CCS (MPa) = N / A (4)

Where N = Maximum Load, A = Area of cross section of pellets

3.4.3 Measurement of biaxial strength of HA Pellets

Biaxial tensile strength involves fracture of samples on application of load along the diameter. The samples were broken in Universal testing machine (UTM) Model H10KS Tinius Olsen. The biaxial strength was calculated using the following formula. [29]

$$\text{Biaxial Strength} = \frac{2P}{\pi dt} \qquad (5)$$

Where, P = Maximum Load, d = Diameter, t = thickness

3.4.4 Specific gravity and total porosity

Specific gravity of powder sample was measured in a pycnometer using the following formula.[30]

M_1 = mass of empty pycnometer

M_2 = mass of pycnometer with sample

M_3 = mass of pycnometer with sample and liquid

M_4 = mass of pycnometer with liquid

$$\text{Specific Gravity} = \frac{M2-M1}{(M4-M1)-(M3-M2)} \qquad (6)$$

$$\text{Total porosity} = \left(1 - \frac{\text{Bulk Density}}{\text{Specific } Gravity}\right) \times 100 \qquad (7)$$

3.4.5 Microstructure analysis by FESEM

The microstructure and porosity of porous HA pellets were studied by Field Emission Scanning Electron Microscope (FESEM). The pellets were gold coated and then loaded for 3minutes in FESEM machine FEI NANO SEM 450 and the pellets were observed in secondary electron (SE) mode at 15KV accelerating voltage.

CHAPTER 4

RESULTS AND DISCUSSION

4.1 Phase analysis of calcined HA

Figure 4.1 shows the X-Ray Diffraction pattern of calcined HA. The HA peaks were identified by referring JCPDS files (74-0565) and the XRD pattern is shown:

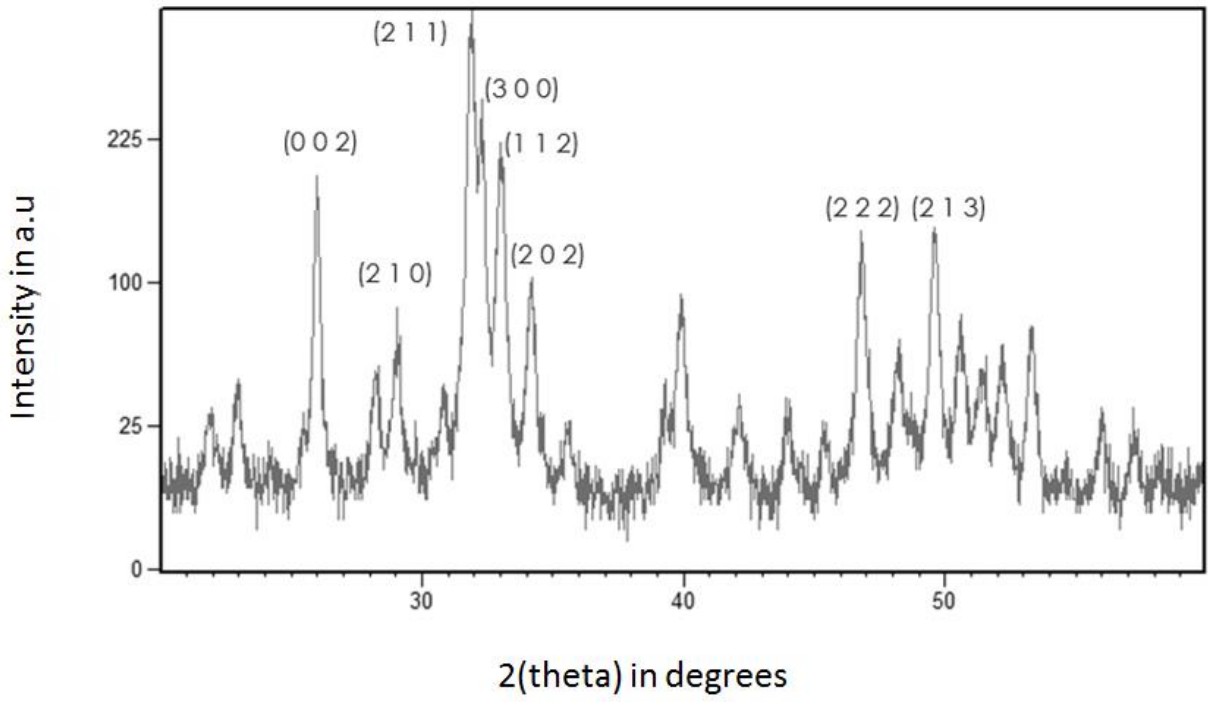

Fig 4.1 X-Ray Diffraction pattern of calcined HA at 850^0C

The XRD pattern confirms that major peaks pertain to HA. This implies that the major phase is Hydroxyapatite.

4.2 Bulk density, porosity of HA pellets

Table 4.1 Bulk Density, Apparent porosity of HA pellets with volume% of Plantago ovata and corresponding sample ID

SI No	Sample ID	Volume Percentage Of Plantago ovata	Bulk Density (g/cc)	Apparent Porosity (%)
1	H 100 P0	0	2.13	27.88
2	H 99.5 P0.5	1.1	2.06	28.30
3	H 99 P01	2.2	2.03	30.31
4	H95 P05	10.5	1.92	34.57
5	H90 P10	20	1.80	38.13
6	H85 P15	28	1.63	40.62
7	H80 P20	36	1.51	42.62

The effect of addition of Plantago ovata as a pore former to the HA on bulk density and apparent porosity is shown in the Table 4.1. The porosity and bulk density were dependent on percentage of pore formers. With increase in pore formers, the porosity increases. However the porosity increase is more pronounced for higher pore former concentration.

The graph 4.2 shows the bulk density value is stepping down from 2.13 to 1.51 g/cc with increasing Plantago ovata volume % in HA pellets

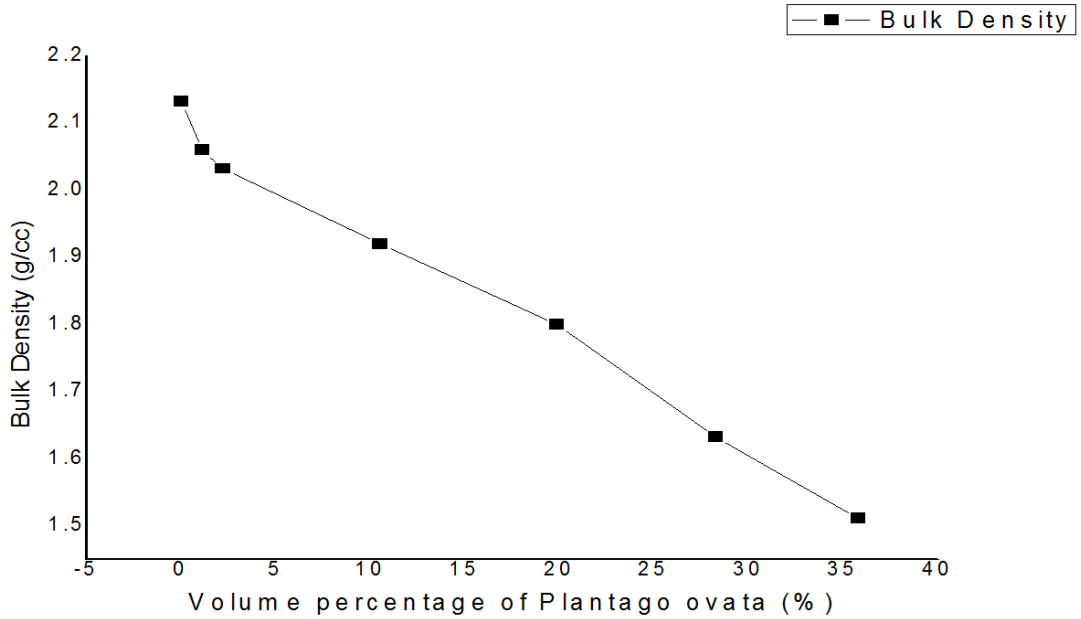

Fig 4.2 Graph between bulk densities of HA pellets with volume% of Plantago ovata

The graph 4.3 shows how the apparent porosity of HA Pellets is increasing with increasing Plantago ovata volume % in HA pellets.

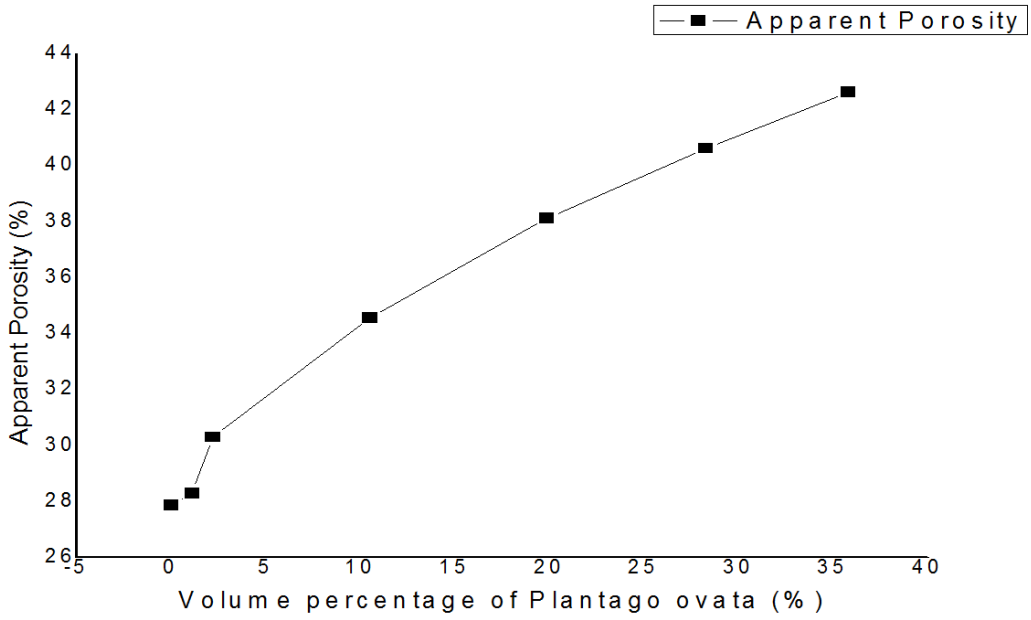

Fig 4.3 Graph between Apparent Porosities of HA pellets with volume% of Plantago ovata

4.3 Cold Crushing Strength of HA Pellets

The effect of increasing Plantago ovata in the HA pellets is reflected on compressive strength of samples (Table 4.2).

Table 4.2 Cold Crushing Strength of HA pellets with volume% of Plantago ovata and corresponding sample ID

SI No	Sample ID	Volume Percentage Of Plantago ovata	CCS (MPa)
1	H 100 P0	0	56.53
2	H 99.5 P0.5	1.1	56.18
3	H 99 P01	2.2	55.85
4	H95 P05	10.5	51.57
5	H90 P10	20	40.64
6	H85 P15	28	21.293
7	H80 P20	36	3.795

This can be explained as the presence of pores affect the strength of materials. After the burn out of Plantago ovata large pores remain in the structure hence it results in higher porosity of HA pellets. With increase in the volume of pore former strength decreases. Maximum strength is obtained at pure HA pellets having no pore fomer and minimum strength is obtained at H80P20 wher 35 volume % of pore former is used.

Figure 4.4 shows that cold crushing strength decreases with increasing Plantago ovata.

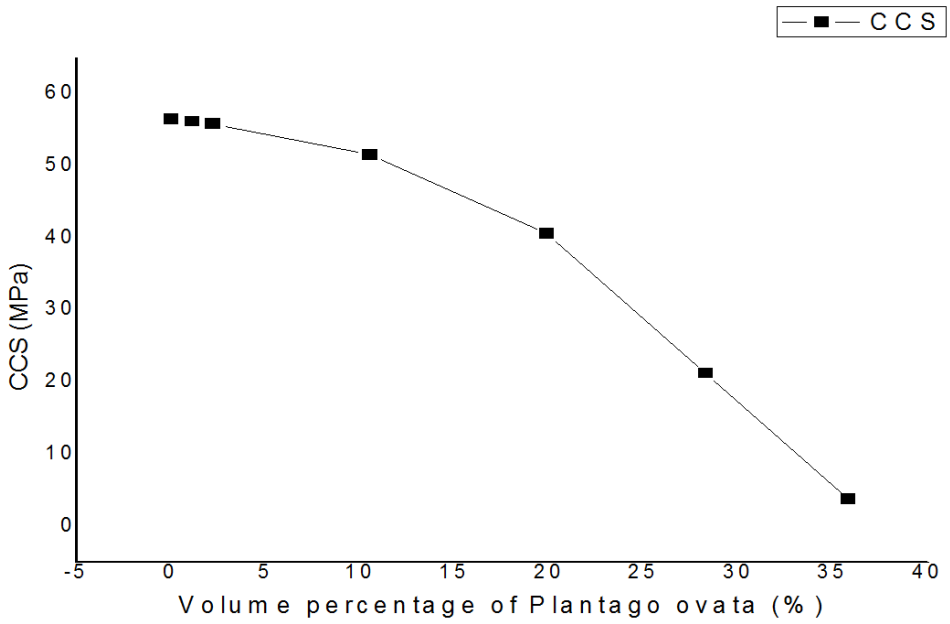

Fig 4.4 Graph between CCS of HA pellets with volume% of Plantago ovata

4.4 Biaxial Strength of HA Pellets

Table 4.3 Biaxial Strength of HA pellets at 1250^{0}C and 1300^{0}C with volume% of Plantago ovata and corresponding sample ID

SI No	Sample ID	Volume Percentage Of Plantago ovata	Strength (MPa) For Pellets fired at 1250^{0}C , 1Hr	Strength (MPa) For Pellets fired at 1300^{0}C , 1Hr
1	H 100 P0	0	18.58	21.32
2	H 99.5 P0.5	1.1	17.64	20.94
3	H 99 P01	2.2	17.13	20.57
4	H95 P05	10.5	14.14	16.46
5	H90 P10	20	10.71	12.83
6	H85 P15	28	6.7	8.26
7	H80 P20	36	4.2	5.74

Biaxial strength also depend upon the pores in a material. After the burn out of pore formers large pores remain in the structure hence it results in higher porosity of HA pellets. With increase in the volume of pore former biaxial strength decreases. Maximum strength is obtained at pure HA pellets having no pore fomer and minimum strength is obtained at H80P20 wher 35 volume % of

pore former is used. Fig 4.5 and Fig 4.6 shows the variation of biaxial strength with respect to volume % of Plantago ovata in HA for pellets fired at 1250^0Cand 1300^0C respectively.

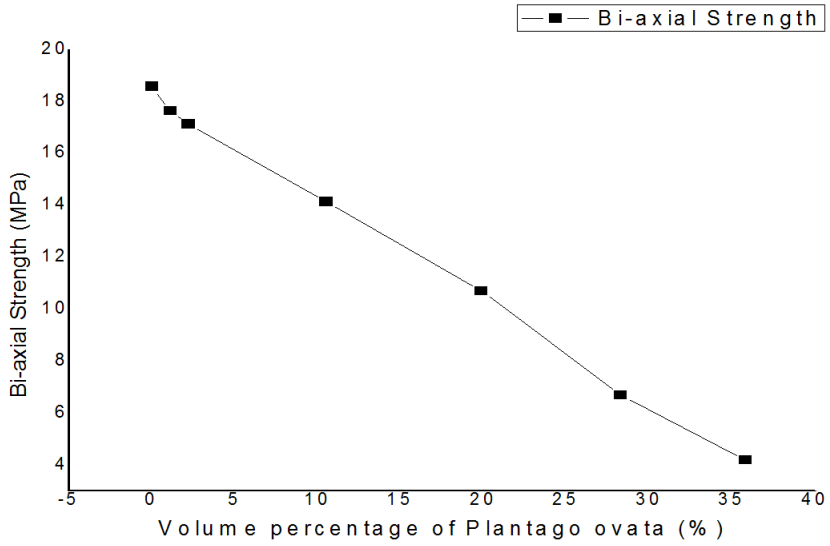

Fig 4.5 Biaxial strength of HA pellets fired at 1250 ^{0}C vs volume% of Plantago ovata

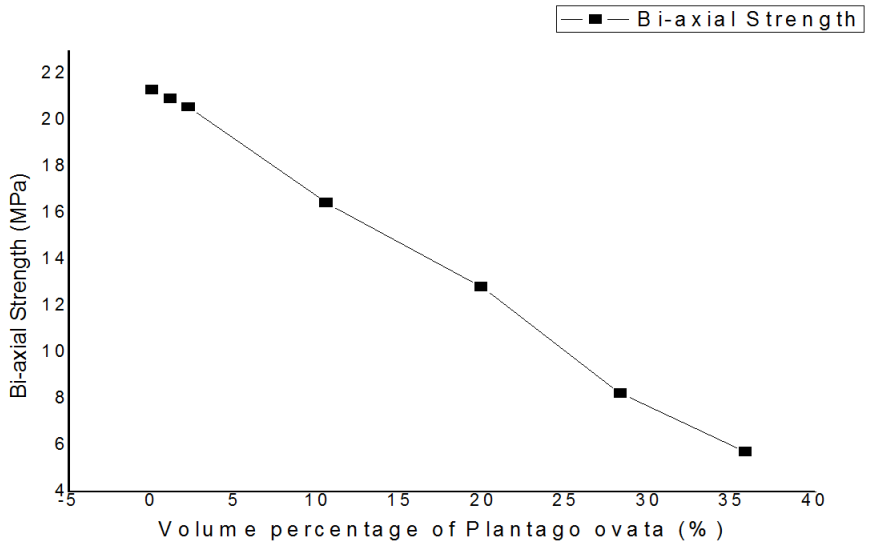

Fig 4.6 Biaxial strength of HA pellets fired at 1300 ^{0}C vs volume% of Plantago ovata

4.5 Specific Gravity and Total Porosity of sintered HA

Table 4.4 Specific gravity of ground HA powder

Sample	I	II	III	IV	V	VI	VII	Average
SG	3.014	3.0169	2.991	3.0016	3.07	3.022	3.0168	3.0189

Table 4.4 shows the average specific gravity of ground HA powder which was found to be 3.0189 by pycnometer experiment.

Table 4.5 Total Porosity of HA with volume% of Plantago ovata and corresponding sample ID

SI No	**Sample ID**	**Volume Percentage Of Plantago ovata**	**SG of ground powder**	**Total Porosity(%) = (**1- BD/SG)×100
1	H 100 P0	0	3.0189	29.36
2	H 99.5 P0.5	1.1		31.76
3	H 99 P01	2.2		32.69
4	H95 P05	10.5		36.40
5	H90 P10	20		40.37
6	H85 P15	28		45.90
7	H80 P20	36		49.90

The effect of addition of Plantago ovata as a pore former to the HA on total porosity is shown in the table 4.5. After the burn out of pore formers large pores remain in the structure which leads to higher porosity of HA pellets.

The graph in Figure 4.7 shows the variation of porosity. It is increasing with increasing Plantago ovata volume % in HA pellets fired at 1250 ^{0}C.

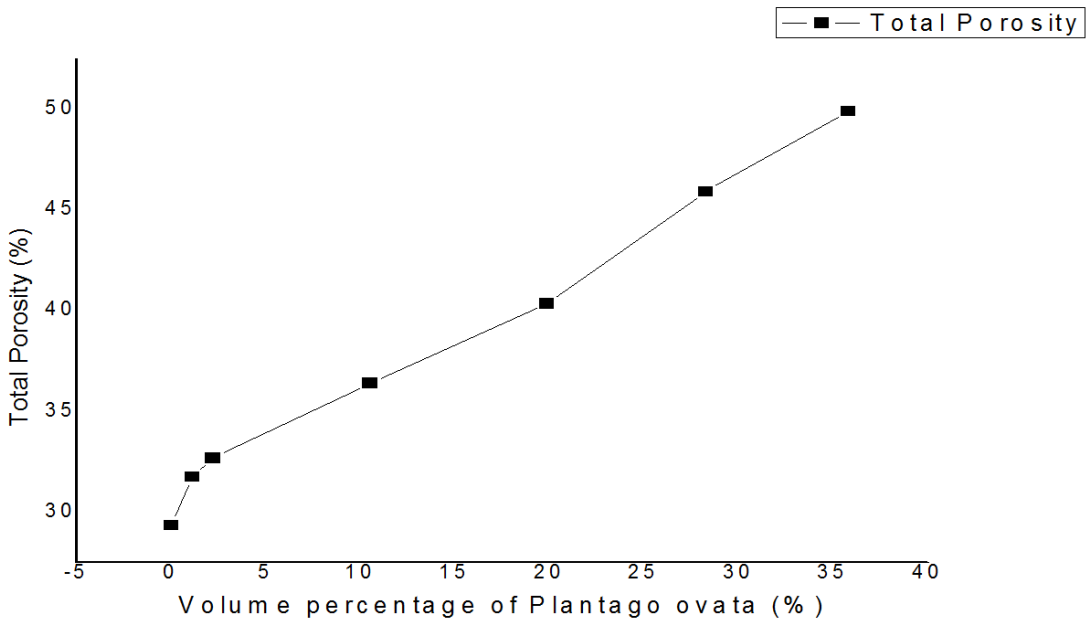

Fig 4.7 Graph between total porosities of HA pellets with volume% of Plantago ovata

4.6 Microstructure of the porous HA pellets

Fig-4.8 shows the FESEM images of porous HA Pellets. Micro and macropores were observed in the surface of pellets. Larger pores in the range of 50-100 micrometer were observed in the porous HA pellets. Larger pores are because of the burn out of the Plantago ovata particles. The FESEM images are exhibited below:

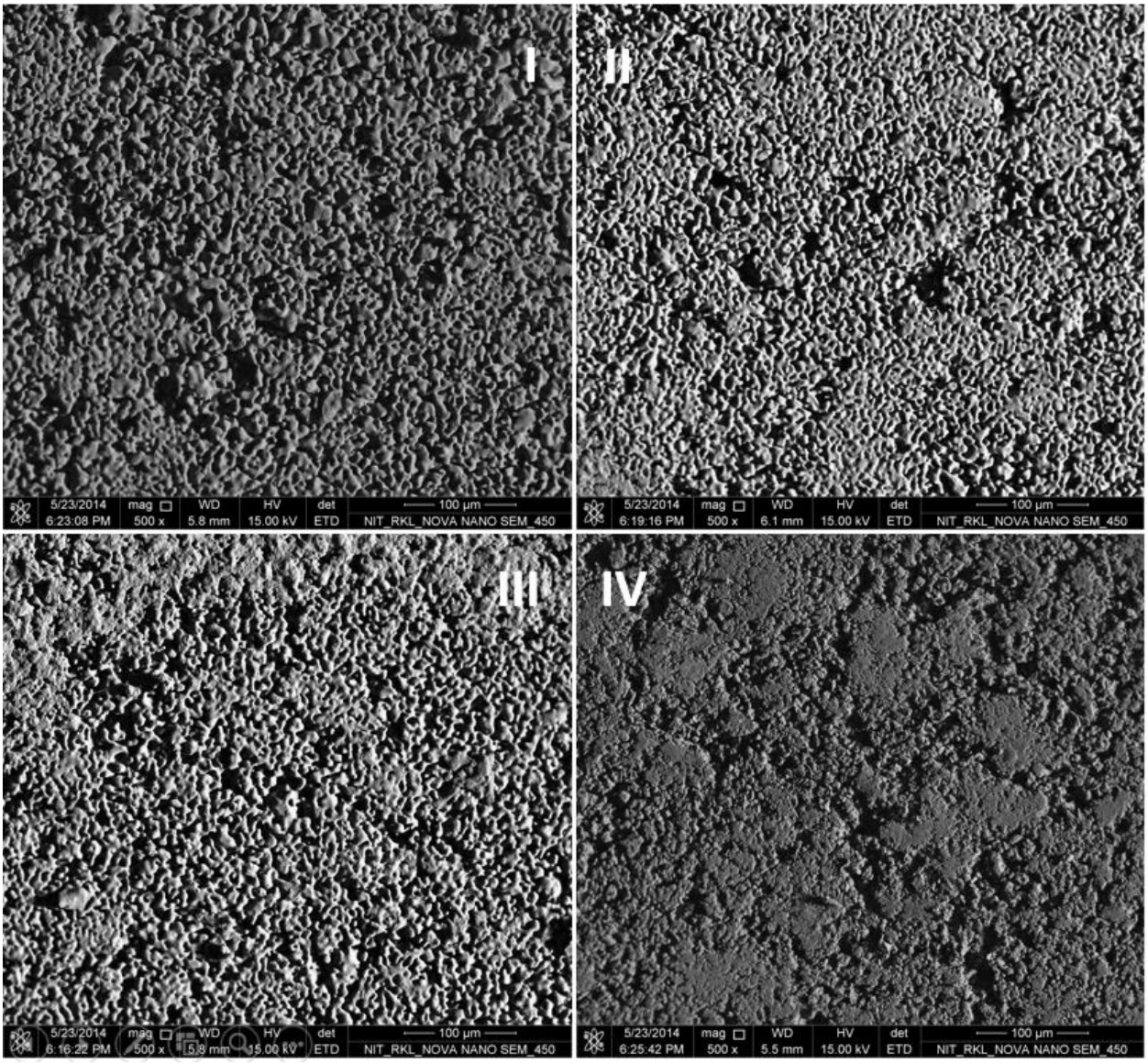

Fig-4.8 FESEM of porous HA pellets for (I) Sample H99.5 P0.5, (II) Sample H99 P01, (III) Sample H95P05, (IV) Sample H90P10

From the FESEM image of porous HA pellets it was seen that the porosity of the pellets depends on the amount of pore former added in the batch of porous HA. Higher the pore former percentage, higher % of porosity was observed for porous HA.

CHAPTER 5

CONCLUSIONS

CONCLUSIONS

- The Hydroxyapatite prepared from Ca(NO3)2.4H2O and $(NH_4)_2HPO_4$ and was calcined at 850^0C. The XRD analysis showed the presence Hydroxyapatite as major phase.
- The porous Hydroxyapatite pellets were prepared by using Plantago ovata as pore former and PVA as binder (3%). Pellets were fired at 1250^0C and 1300^0C for 1 Hr.
- In porous Hydroxyapatite pellets fired at 1250^0C for 1 Hour, the bulk density decreased (2.13g/cc to 1.5g/cc) with an increase in 0 to 35 volume % Plantago ovata content.
- In porous Hydroxyapatite pellets, the apparent porosity increased (27% to 43%) with an increase in Plantago ovata content varying from 0 to 35 volume % of it.
- In porous Hydroxyapatite pellets fired at 1250^0C for 1 Hour, the cold crushing strength decreased (from 56 MPa to 4 MPa) and Biaxial tensile strength decreased (from 18 MPa to 4 MPa) with an increase in 0 to 35 volume % Plantago ovata content.
- In porous Hydroxyapatite pellets fired at 1300^0C for 1 Hour, the biaxial strength decreased (from 21 MPa to 5 MPa) with an increase in 0 to 35 volume % content.
- In porous Hydroxyapatite pellets, the total porosity increased (from 29% to 49%) with an increase in Plantago ovata content varying from 0 to 35 volume % of it.
- In porous HA pellets FESEM images exhibited that the porosity of the pellets depends on the amount of pore former added in the batch of porous HA. Higher the pore former percentage, higher % of porosity was observed for porous HA.

ABBREVIATIONS

- HA: Hydroxyapatite
- HAP: Hydroxyapatite Powder
- TCP: Tricalcium Phosphate
- AP: Apparent Porosity
- BD: Bulk Density
- PVA: Poly Vinyl Alcohol
- CCS: Cold Crushing Strength
- XRD: X-Ray Diffractometer/ X-Ray Diffraction
- FESEM: Field Emission Scanning electron microscope
- SG: Specific Gravity
- TP: Total Porosity

REFERENCES

1. P Sepulveda, J Binner, S Rogero, O Higa, J Bressiani,"Production of porous hydroxyapatite by the gel-casting of foams and cytotoxic evaluation", J Biomed Mater Res. 2000 Apr, 50(1):27-34
2. G Meng , H Wang , W Zheng, X Liu,"Preparation of porous ceramics by gelcasting approach", Mater Lett 45 2000 224–227
3. P Greil,"Near net shape manufacturing of ceramics" , J Mat Chem and Phys 61 (1999) 64-68
4. K Leong, C Cheah, C Chua , "Solid freeform fabrication of three-dimensional scaffolds for engineering replacement tissues and organs", J Biomat 24 (2003) 2363–2378
5. L Montanaro, Y Jorand, G Fantozzi and A. Negro, "Ceramic Foams by Powder Processing", J Euro Ceram Soc , 18 (1998) 1339-1350
6. B Nait-Ali, K Haberko, H Vesteghem, J Absi, D Smith, "Thermal Conductivity of highly porous zirconia", J Euro Ceram Soc 26 (2006)
7. L Hu, C Wang, Y Huang, "Porous yttria-stabilized zirconia ceramics with ultra-low thermal conductivity", J Mater Sci (2010) 45:3242–3246
8. J She and T Ohji,"Thermal Shock Behavior of Porous Silicon Carbide Ceramics", J Am Ceram Soc , 85 [8] 2125–27 (2002)
9. C Effting, O Alarcon, S Güths, A Oliveira, J Paschoal , "Influence of porosity on thermal properties of ceramic floor tiles", J Qualicer 2006
10. United States Patent, Komoda, Patent Number, 4810,273,"Porous Ceramic Filter", Patent Date: Mar. 7, 1989

11. X Huang, “Separator technologies for lithium-ion batteries”, J Solid State Electrochem (2011) 15:649–662
12. United States Patent, Patent Number, 3021,379, “Ceramic Separators for primary batteries”, Patent Date: Feb. 13, 1962
13. M Dias, P Fernandes, J Guedes, S Hollister, “Permeability analysis of scaffolds for bone tissue engineering” , J Biomech 45 (2012) 938-944
14. W Suchanek and M Yoshimura, “Preparation of Fibrous, Porous Hydroxyapatite Ceramics from Hydroxyapatite Whiskers”, J Am Ceram Soc, 81 [3] 765–67 (1998)
15. A Singh, “Hydroxyapatite, a biomaterial: Its chemical synthesis, characterization and study of biocompatibility prepared from shell of garden snail, Helix aspersa”, Bull. Mater. Sci., Vol. 35, No. 6, November 2012, pp. 1031–1038. Indian Academy of Sciences.
16. I. Sopyan, M Mel, S. Ramesh, K Khalid, “Porous hydroxyapatite for artificial bone applications”, Science and Technology of advanced materials, 8 (2007) 116-123
17. V Orlovskii, V Komlev, S Barino, “Hydroxyapatite and Hydroxyapatite-Based Ceramics”, Inorganic Materials, Vol. 38, No. 10, 2002, pp. 973–984
18. R Schnettler, V Alt, E Dingeldein, H Pfefferle, O Kilian,, C Meyer, C Heiss, S Wenisch,“Bone ingrowth in bFGF-coated hydroxyapatite ceramic implants”, Biomaterials 24 (2003) 4603-4608
19. L Jongpaiboonkit, T Franklin-Ford, and W Murphy, “Mineral-Coated Polymer Microspheres for controlled Protein Binding and Release”, J Advanced Materials 2009, 21, 1960–1963

20. H Oonishi, M Yamamoto, H Ishimaru, E Tsuji, S Kushitani, M Aono, Y Ukon , "The effect of hydroxyapatite coating on bone growth into porous titanium alloy implants", The journal of bone and joint surgery, vol. 71-B. No. 2. March 1989
21. R Thomson, M Yaszemski, J Powers, A Mikos, "Hydroxyapatite fiber reinforced poly (alpha-hydroxy ester) foams for bone regeneration", J Biomaterials 19 (1998) 1935—1943
22. A Chetty, I Wepener, MMarei, YKamary, R Moussa, "Hydroxyapatite: synthesis, properties, and applications" Polymers and composites, Materials science and manufacturing
23. H Kim, J Knowles, H Kim, "Hydroxyapatite/ Poly caprolactone composite coatings on hydroxyapatite porous bone scaffold for drug delivery", J Biomaterials 25 (2004) 1289-1287
24. YJ Tang, YF Tang, C Lv, Z Zhou, "Preparation of uniform porous hydroxyapatite biomaterials by a new method", J Applied Surface Science 254 (2008) 5359–5362
25. S Deville, E Saiz and A Tomsia, "Freeze casting of hydroxyapatite scaffolds for bone tissue engineering", J Biomaterials 27 (2006) 5480-5489
26. S Kwon, Y Jun, S Hong, I Lee, and H Kim; "Calcium phosphate bioceramics with various porosities and dissolution rate" J Am Ceram Soc 85[12] 3129-31(2002).
27. ASTM international, C830 - 00(2011) ,Standard Test Methods for Apparent Porosity, Liquid Absorption, Apparent Specific Gravity, and Bulk Density of Refractory Shapes by Vacuum Pressure
28. James S Reed, 2nd Edition, Principles of Ceramic Processing, Equation 15.20
29. James S Reed, 2nd Edition, Principles of Ceramic Processing, Equation 15.21

30. ASTM international , D70 - 09e1 , D70 Standard Test Method for Density of Semi-Solid Bituminous Materials (Pycnometer Method)